

Supplementary Materials for

Pain induces stable, active microcircuits in the somatosensory cortex that provide a therapeutic target

Takuya Okada, Daisuke Kato, Yuki Nomura, Norihiko Obata, Xiangyu Quan, Akihito Morinaga, Hajime Yano, Zhongtian Guo, Yuki Aoyama, Yoshihisa Tachibana, Andrew J. Moorhouse, Osamu Matoba, Tetsuya Takiguchi, Satoshi Mizobuchi, Hiroaki Wake*

*Corresponding author. Email: hirowake@med.nagoya-u.ac.jp

Published 19 March 2021, *Sci. Adv.* 7, eabd8261 (2021)

DOI: 10.1126/sciadv.abd8261

The PDF file includes:

Figs. S1 to S10
Legends for movies S1 and S2
Legend for data file S1

Other Supplementary Material for this manuscript includes the following:

(available at advances.sciencemag.org/cgi/content/full/7/12/eabd8261/DC1)

Movies S1 and S2
Data file S1

Supplementary Materials:

Supplementary Figures

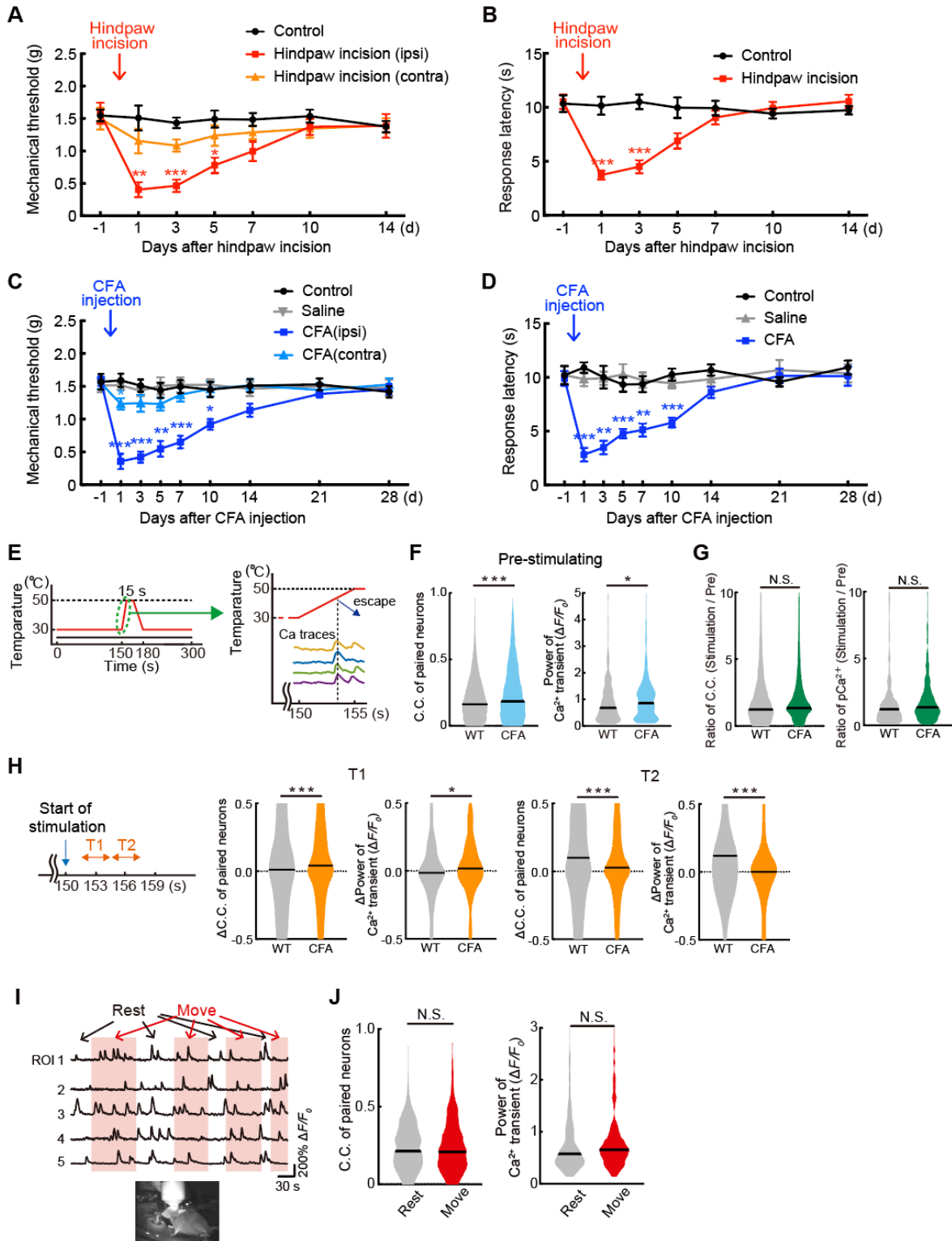


Fig. S1. Behavioral evaluation of two mouse pain models and Supplement to the experiment in Fig.1. (A, B) Postoperative pain model. (C, D) Inflammatory pain model. (A) Mechanical threshold to von Frey filaments. (black, control ($n = 7$ mice); red, hind paw incision [ipsilateral] ($n = 7$ mice); orange, hind paw incision [contralateral] ($n = 7$ mice)). (B) Withdrawal response latency to hot plate test (black, control ($n = 7$ mice); red, hind paw incision ($n = 7$ mice)). (C) Mechanical threshold to von Frey filaments (black, control ($n = 7$ mice); gray, saline injected control ($n = 7$ mice); blue, CFA [ipsilateral] ($n = 7$ mice); right blue, CFA [contralateral] ($n = 7$ mice)). (D) Withdrawal response latency to hot plate test (black, control ($n = 7$ mice); gray, saline injected control ($n = 7$ mice); blue, CFA ($n = 7$ mice)). $*P < 0.05$, $**P < 0.01$, $***P < 0.001$, by two-way ANOVA followed by Bonferroni test, vs control. In all graphs, data and error bars show mean \pm SEM. (E) Schematic diagram of thermal stimulation applied to right hind paw of mice, and the relative timing of neural activity imaging and the typical escape responses, measured simultaneously by a CCD camera. (F) Direct comparison of the baseline absolute C.C. and pCa^{2+} values between WT ($n = 14,257$ pairs, 372 neurons / 5 mice) and inflammatory pain model (CFA) mice ($n = 12,847$ pairs, 357 neurons / 5 mice). Data derived from the pre-stimulation (baseline) period shown in Fig. 1. $*P < 0.05$, $***P < 0.001$, by Mann-Whitney U test. (G) Direct comparison of the relative stimulation induced changes (Stimulation / Pre) in C.C. and pCa^{2+} values between WT ($n = 14,257$ pairs, 372 neurons / 5 mice) and CFA mice ($n = 12,847$ pairs, 357 neurons / 5 mice) using the data from Fig.1. N.S., not significant, by Mann-Whitney U test. Violin plots in F and G show median (black line) and distribution of the data. (H) Temporal pattern of changes in C.C. and pCa^{2+} in WT ($n = 277$ neurons / 5 mice) and CFA mice ($n = 268$ neurons / 5 mice) when analysed every 3 seconds from the start of thermal stimulation, using the data shown in Fig.1 but only neurons that responded to the stimulation were analysed. Data shows the reduced latency of responses in CFA mice. $*P < 0.05$, $***P < 0.001$, by Mann-Whitney U test. Violin plots show median (black line) and distribution of the data. (I) Calcium traces of five typical neurons measured during periods of rest and movement, as indicated. (J) Comparison of C.C. of paired neurons and pCa^{2+} at rest and movement ($n = 1476$ pairs, 124 neurons / 5 mice). N.S., not significant, by paired t test.

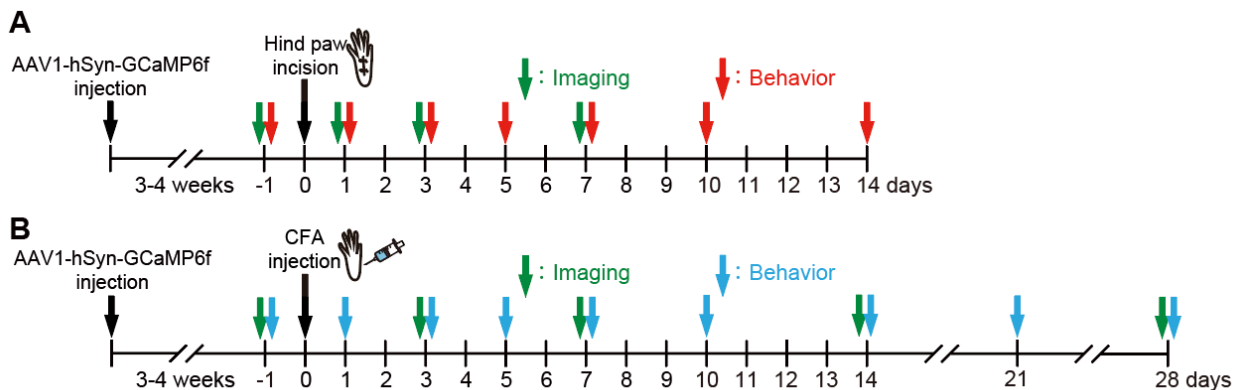


Fig. S2. Experimental protocols in the two mouse pain models.

(A) Experiments started around 3-4 weeks after the virus injection. Right hind paw incision was performed on day 0, Ca^{2+} imaging from left S1HL was repeated on pre, day 1, 3, 7, and behavioral evaluation was performed on pre, day 1, 3, 5, 7, 10, 14 (green arrows, imaging; red arrows, behavior). (B) Experiments started around 3-4 weeks after the virus injection. CFA was injected into right hind paw on day 0. Ca^{2+} imaging from left S1HL occurred one day prior to injection (pre), and again at day 3, 7, 14, 28. Behavioral evaluation was performed on pre, day 1, 3, 5, 7, 10, 14, 21, 28 (green arrows, imaging; blue arrows, behavior).

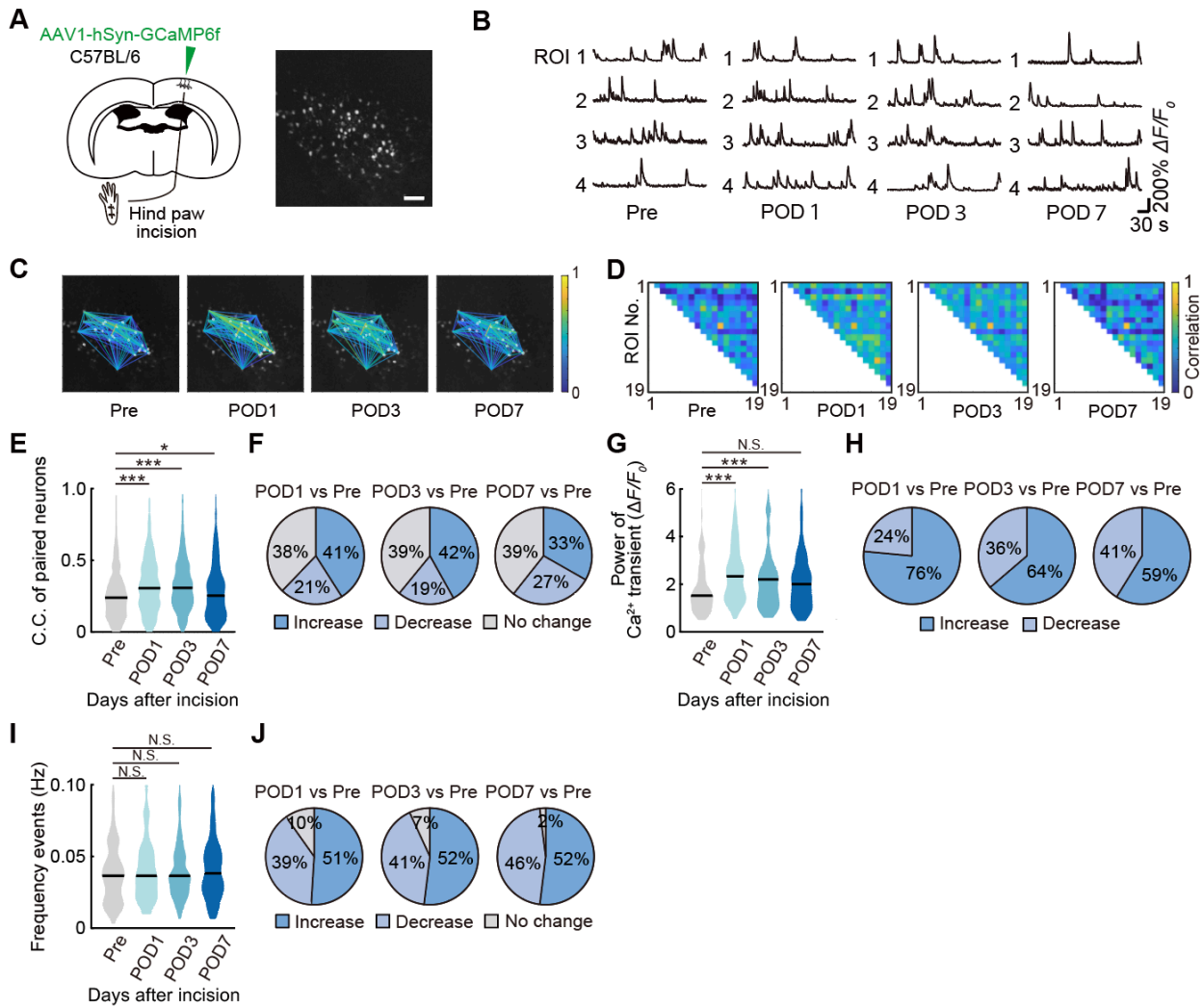


Fig. S3. Tracing of individual spontaneous neuronal activity in postoperative pain model.

(A) Schematic diagram showing virus injection in the hindlimb region of primary somatosensory cortex (S1HL). *In vivo* Ca^{2+} imaging of S1HL neurons. The same neurons were imaged pre and post-hind paw incision (pre and postoperative day 1, 3, 7). Scale bar, 100 μm . (B) Calcium traces of typical four neurons. Each neuronal activity was traced from pre to post-hind paw incision. A representative example of paired neuronal C.C. from pre to post-hind paw incision. (C, D) A representative example of paired neuronal C.C. from pre to post-hind paw incision. (E, G, I) C.C. of paired neurons ($n = 737$ pairs / 7 mice), power of Ca^{2+} transients (pCa^{2+}) and frequency of Ca^{2+} transients ($n = 102$ neurons / 7 mice) from pre to post-hind paw incision. N.S., not significant, $*P < 0.05$, $***P < 0.001$, by paired t test. Violin plots show median (black line) and distribution of the data. (F, H, J) Change in C.C. of paired neurons ($n = 737$ pairs / 7 mice), pCa^{2+} and frequency of Ca^{2+} transients ($n = 102$ neurons from 7 mice) from pre to post-hind paw incision (The increased/decreased correlation coefficient was defined if the difference in values of individual pairs exceeded 0.1).

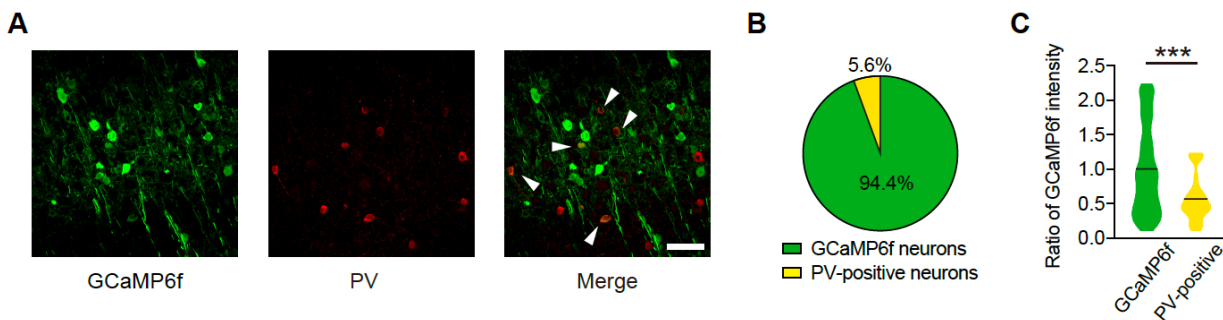


Fig. S4. Proportion of PV neurons in the population of imaged neurons.

(A) GCaMP6f expression (left) and PV immunostaining (middle) from a WT mouse that was injected AAV1-hSyn-GCaMP6f in S1HL. Scale bar, 50 μ m. Arrows represent double positive neurons in GCaMP6f and PV. (B) Proportion of PV-positive neurons (red) out of all GCaMP6f-expressing neurons (22 PV-positive neurons and 393 GCaMP6f-expressing neurons in 8 slices / 4 mice). (C) Ratio of GCaMP6f intensity in all GCaMP6f-expressing neurons and PV-positive neurons. *** $P < 0.001$, by Mann-Whitney U test. Violin plots show median (black line) and distribution of the data.

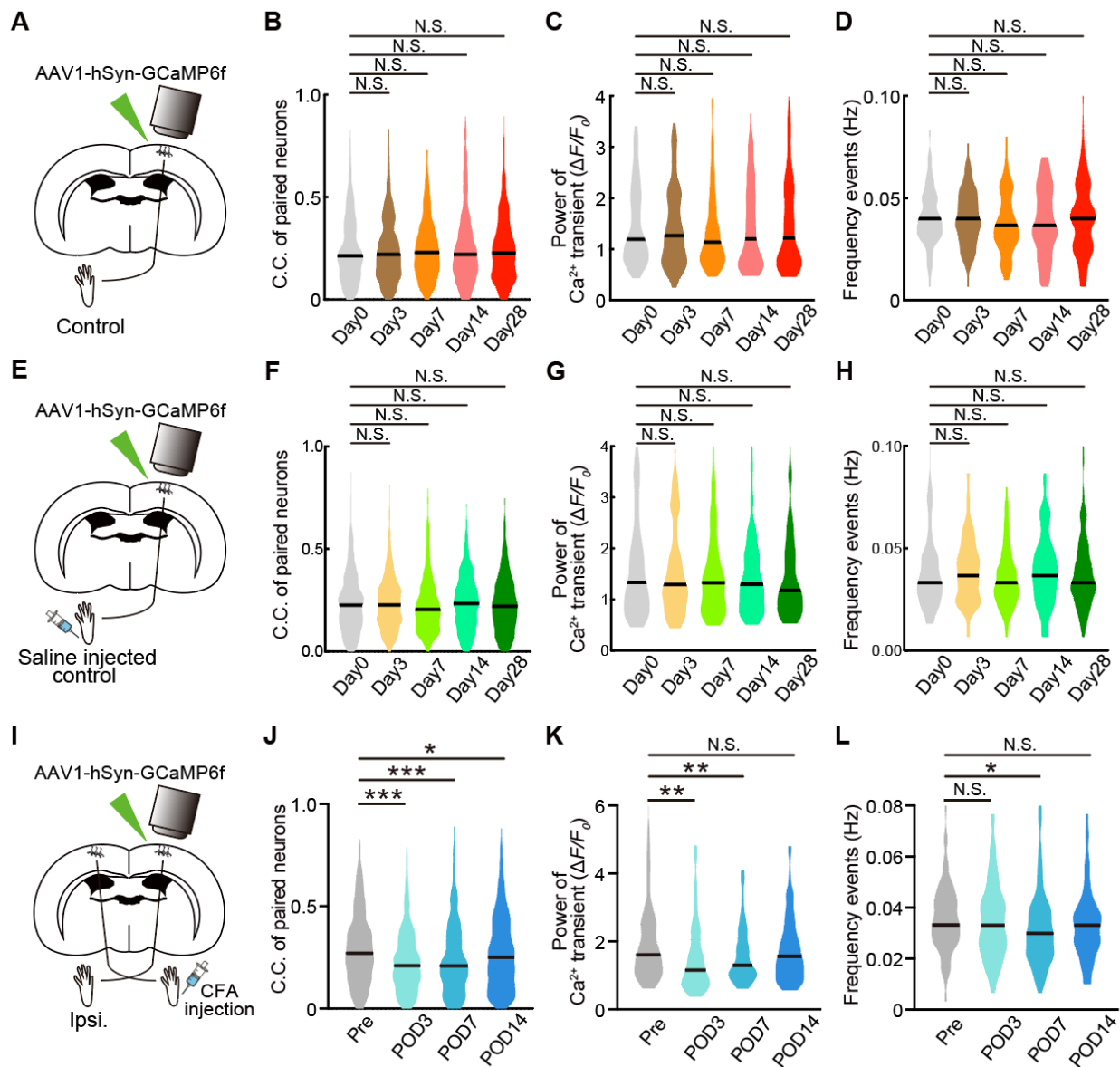


Fig. S5. Tracing of spontaneous neuronal activity in three different control groups: virus controls; saline controls and ipsilateral S1.

Neuronal activity in different control mice was traced over the same time period as for CFA or CNO injected mice in Figs 2-7 of the main paper (0-14 or 28 days). In all relevant panels, violin plots show median (black line) and the distribution of the data. (A) Schematic diagram of the virus control (uninjured mice) experiments. AAV1-hSyn-GCaMP6f was injected into the S1HL of uninjured WT mice to enable *in vivo* Ca^{2+} imaging of S1HL neurons. (B, C, D). C.C. of paired neurons ($n = 548$ pairs / 5 mice), power of Ca transients (pCa^{2+}) and frequency of Ca^{2+} transients ($n = 75$ neurons / 5 mice). N.S., not significant, by paired t test. (E) Schematic diagram of the saline injection control experiments. AAV1-hSyn-GCaMP6f injected into the S1HL in WT mice, and *in vivo* Ca^{2+} imaging of S1HL neurons was repeated over time. Saline was injected once into the right

hind paw using the same approach as in CFA injected mice. (F, G, H) C.C. of paired neurons ($n = 890$ pairs / 5 mice), pCa^{2+} and frequency of Ca^{2+} transients ($n = 89$ neurons / 5 mice) from day 0 to day28 in saline injected control mice. N.S., not significant, by paired t test. (I) Schematic diagram of the ipsilateral S1H control experiments. AAV1-hSyn-GCaMP6f injected into the right S1HL in WT mice to enable *in vivo* Ca^{2+} imaging before and 3-14 days after injection of CFA into the ipsilateral (right) hind paw. (J, K, L) C.C. of paired neurons ($n = 574$ pairs / 5 mice), pCa^{2+} and frequency of Ca^{2+} transients ($n = 78$ neurons / 5 mice) of ipsilateral side of neurons from pre to post-CFA injection (pre, day3, 7, 14). N.S., not significant, $*P < 0.05$, $**P < 0.01$, $***P < 0.001$, by paired t test. Violin plots show median (black line) and distribution of the data.

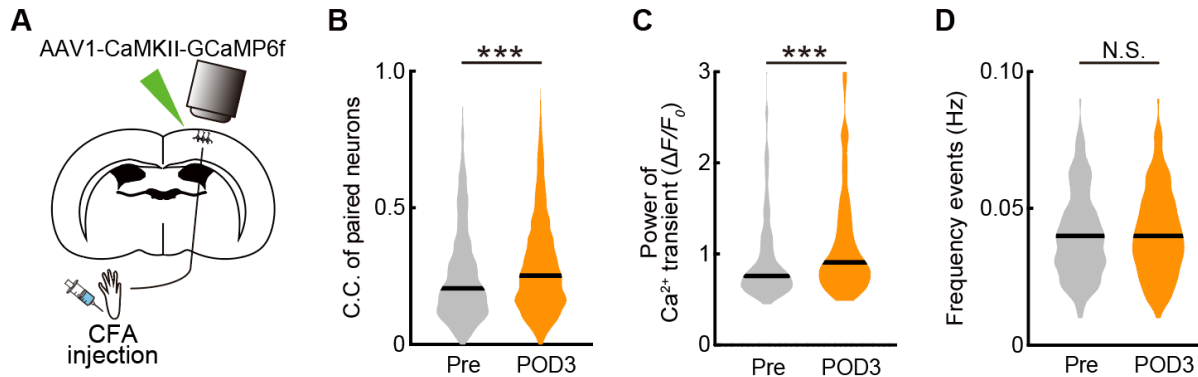


Fig. S6. Tracing of spontaneous neuronal activity in inflammatory pain mice by using the CaMKII promoter to drive GCaMP6f.

(A) Schematic diagram of the control experiment where GCaMP6f was driven by a CAMKII promoter in contrast to the synapsin promoter as used in the main paper (e.g., Figure 2). AAV1-CaMKII-GCaMP6f injected into S1HL in WT mice, *in vivo* Ca^{2+} imaging of S1HL was repeated. The same neurons were imaged pre and post-CFA injection (pre and day 3). (B, C, D) C.C. of paired neurons ($n = 2610$ pairs / 7 mice), pCa^{2+} and frequency of Ca^{2+} transients ($n = 184$ neurons / 7 mice) from pre to post-CFA injection (pre, day3). N.S., not significant, $***P < 0.001$, by paired t test. Violin plots show median (black line) and distribution of the data.

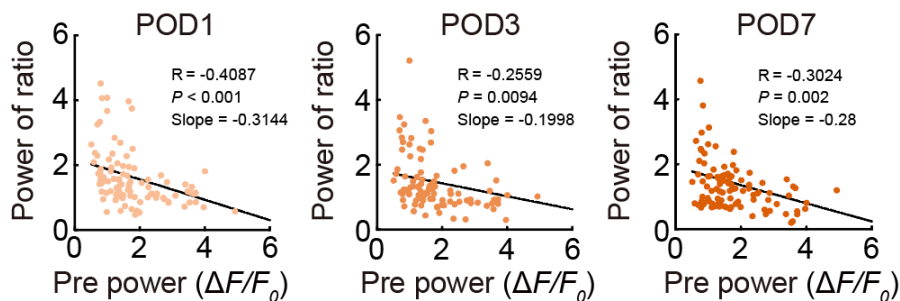


Fig. S7. Neuronal populations responsible for the increased correlation coefficient.

Scatter plot of the relative increase in neuronal pCa^{2+} in each neuron during postoperative pain, plotted against the basal pCa^{2+} before pain, and shown at three different days post operation ($n = 102$ neurons / 7 mice, by Pearson's correlation test).

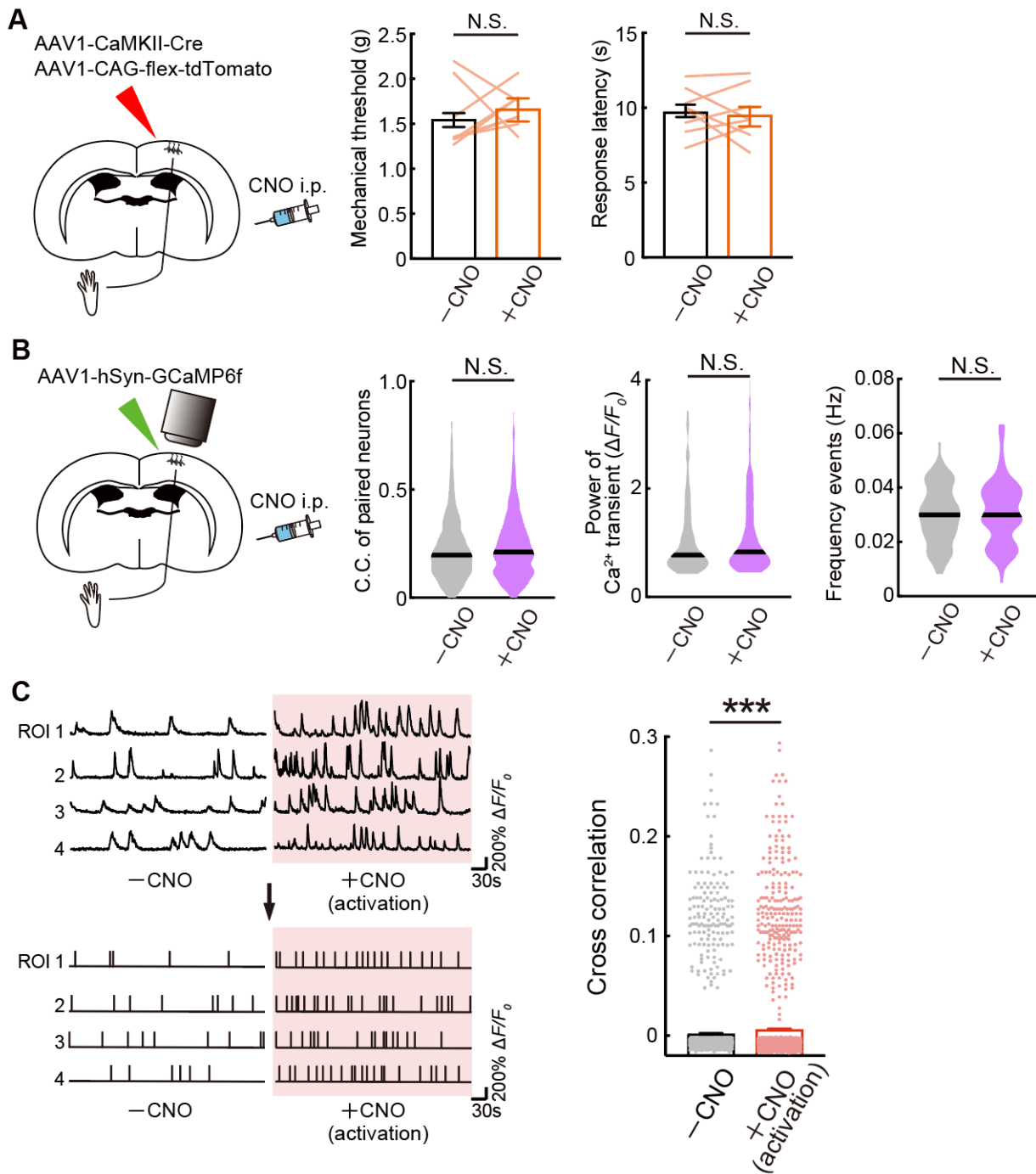


Fig. S8. Control experiments for the chemogenic manipulation data.

(A) Schematic diagram of the virus control experiments, AAV1-CaMKII-Cre and AAV1-CAG-flex-tdTomato viruses (i.e. without the hM3Dq construct) were injected into S1HL in WT mice. Changes in pain threshold pre and post a single dose of CNO were measured ($n = 8$ mice). N.S., not significant, by paired t test. Error bars show mean \pm SEM. (B) Schematic diagram of the CNO control experiments, AAV1-hSyn-GCaMP6f injected into S1HL in WT mice, and *in vivo* Ca^{2+} imaging of S1HL neurons was repeated before (pre) and following a single dose of CNO ($n = 5$ mice) were measured. Change in C.C. of paired neurons ($n = 793$ pairs / 5 mice), power of Ca^{2+} transients ($p\text{Ca}^{2+}$) and frequency of Ca^{2+} transients ($n = 91$ neurons / 5 mice) in pre- and post-CNO. N.S., not significant, by paired t test. Violin plots show median (black line) and distribution of the data. (C) Ca^{2+} transients before and after a single CNO dose in the chemogenic experiments of Fig. 5G-I were re-analysed using a threshold detection to convert to a digitized response of 0 or 1 to negate possible effects of changes in transient duration. The graph shows the subsequent cross correlation data in pre- and post-single dose of CNO. *** $P < 0.001$, by paired t test. All point plots and box plots (mean \pm SEM.) are shown ($n = 2290$ pairs / 5 mice).

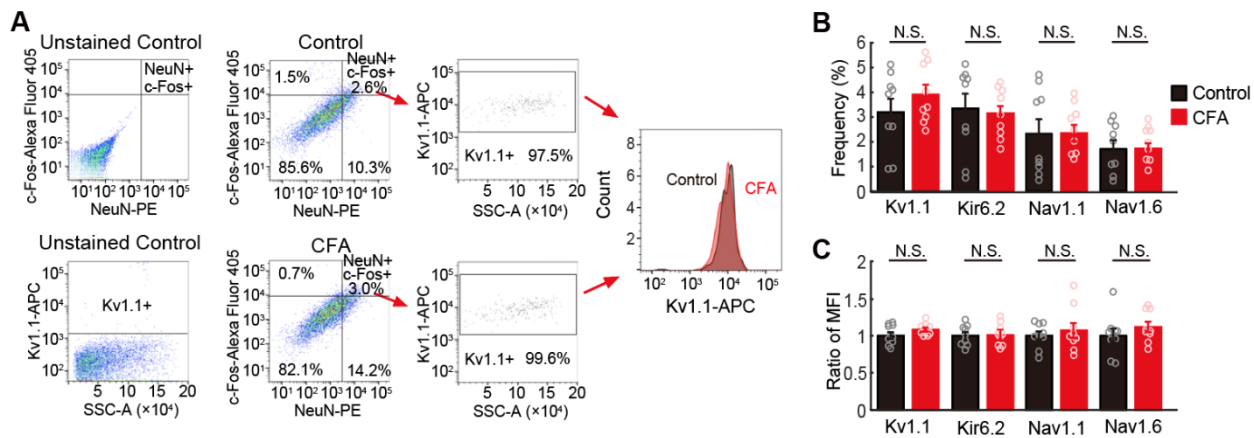


Fig. S9. Comparison of expression of potassium and sodium ion channel subunits in SIHL of control and inflammatory pain model mice.

(A) A representative example of FACS pseudo-color plot. Removal of doublets and debris was performed. Each experiment was obtained from 10^4 cells. The gate for FACS sorting was determined by referring to the unstained control, neurons are gated from non-neurons based on the expression of NeuN-PE, and active neurons are gated from inactive neurons based on the expression of c-Fos-Alexa Fluor 405. Kv1.1-APC (potassium ion channel) positive neurons are gated/counted in active neurons in control (non-injured) and inflammatory pain model mice (3 days after CFA injection). Histogram of expression of Kv1.1 in NeuN, c-Fos and Kv1.1-triple positive neurons in both models (black, control; red, CFA). (B) Frequency of NeuN, c-Fos and each ion channel-triple positive neurons for various potassium and sodium ion channel subunits in cells gated in panel (A) (black, control; red, CFA, $n = 9$ mice for each). N.S., not significant, by unpaired t test. Error bars show mean \pm SEM. (C) The ratio of Mean Fluorescence Intensity (MFI) of each ion channel subunit in NeuN, c-Fos-double positive neurons in inflammatory pain model mice compared with control mice (black, control; red; CFA, $n = 9$ mice for each). N.S., not significant, by unpaired t test. Error bars show mean \pm SEM.

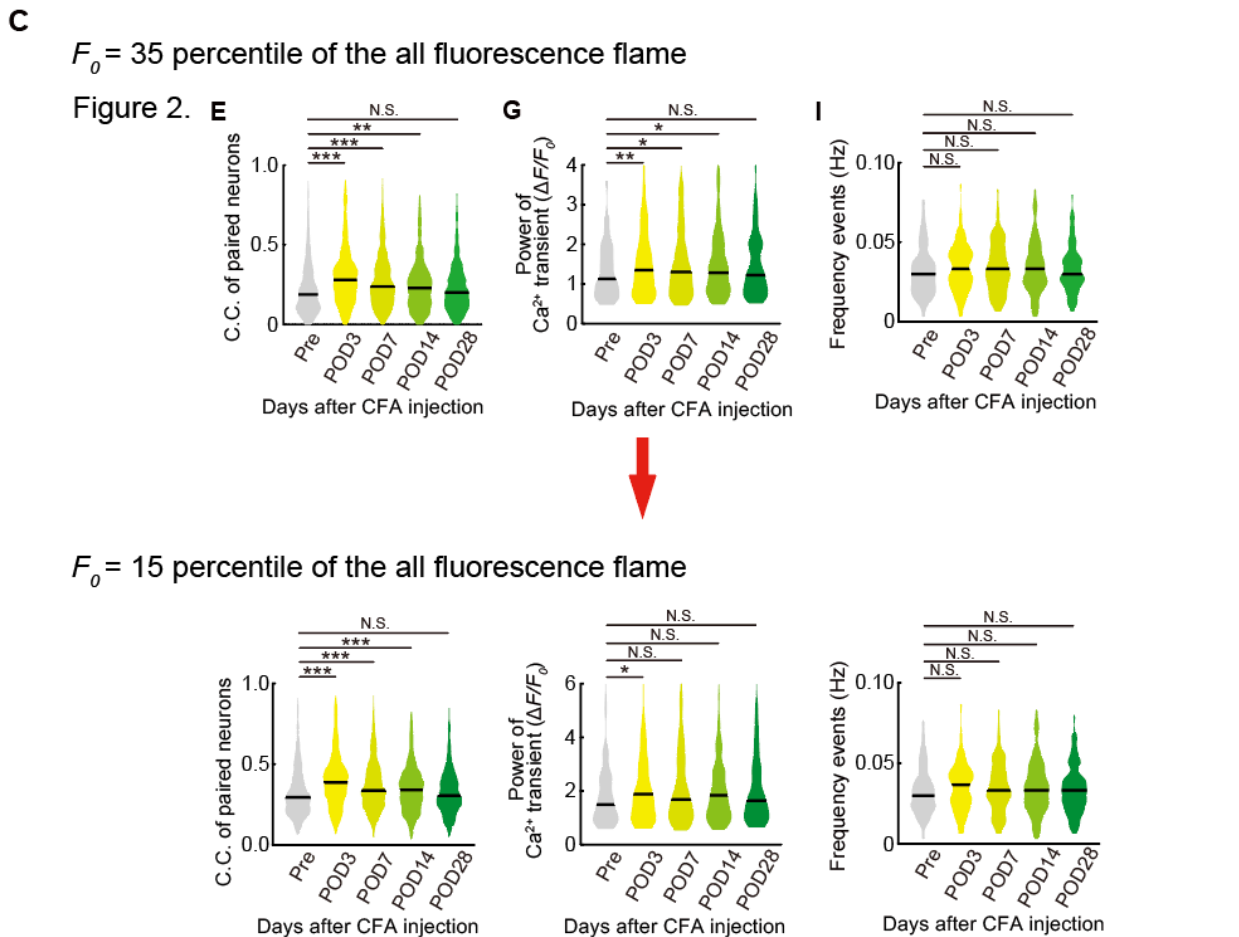
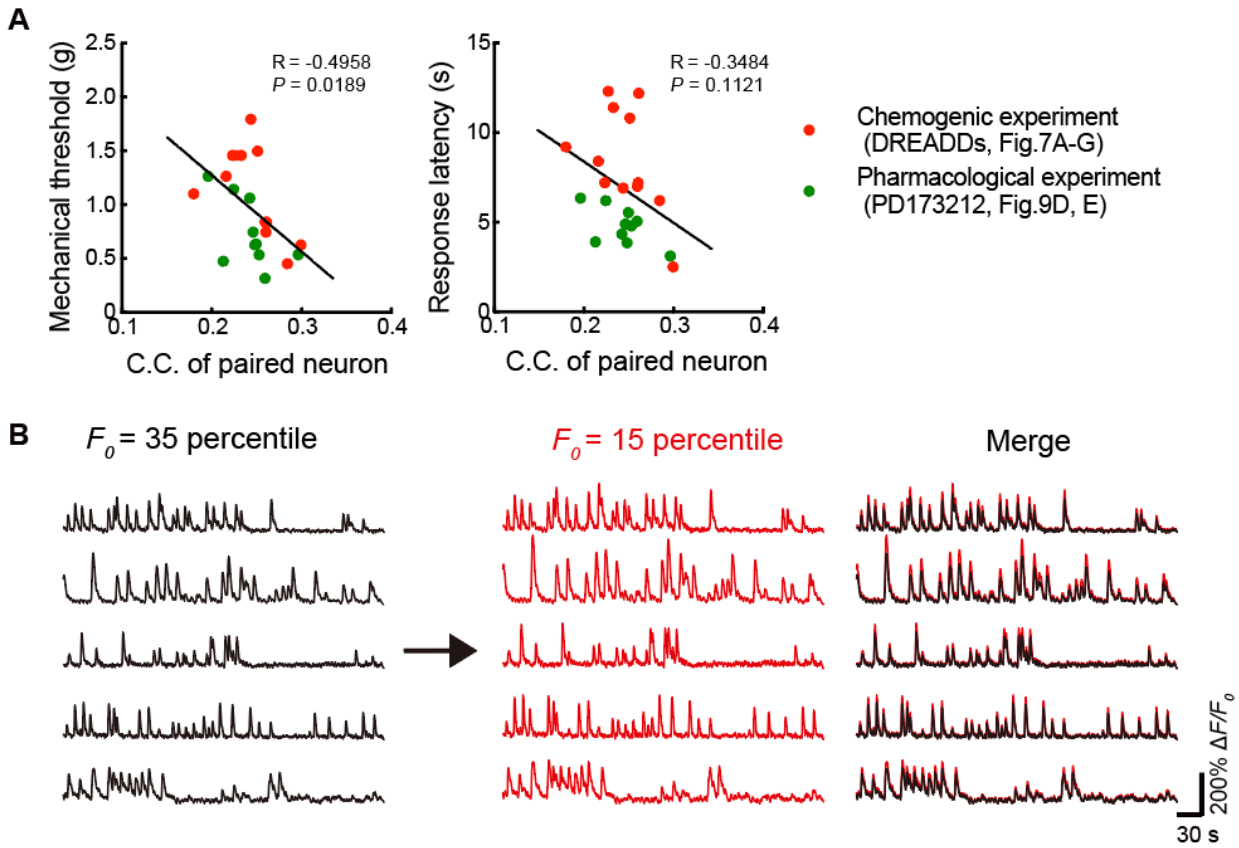


Fig. S10. The correlation between correlation coefficient (C.C.) of paired neurons and pain thresholds, and Ca²⁺ transient parameters detected using a different threshold.

(A) Scatterplots showing the correlation between C.C. and the Mechanical (left) or thermal (right) thresholds using the data from the chemogenic experiments (red, Fig. 7A-G, $n = 4$ mice) and the pharmacological experiments (green, Fig. 9D, E, $n = 5$ mice). Data was fit with a regression using Pearson's correlation test. (B) Comparison of Ca²⁺ transient data when baseline fluorescence was defined as the 35th percentile (left) or 15th percentile (middle) of the total fluorescence intensity histogram obtained during all imaging periods (F_0). (C) Distribution of Ca²⁺ transient parameters compared when using an F_0 of the 35th percentile (as in Fig. 2E, G, I of the main paper) and when using an F_0 of the 15th percentile of the total fluorescence intensity histogram (643 pairs, 97 neurons / 7 mice). N.S., not significant, * $P < 0.05$, ** $P < 0.01$, *** $P < 0.001$, by paired t test. Violin plots show median (black line) and distribution of the data.

Supplementary Movies.

Movie S1.

Representative *in vivo* two-photon images of S1HL neurons pre- and post-administration of PD173212 in CFA-injected mice (3 days after the injection). The same cells were traced. Scale bar; 100 μm , play at 10 times speed (1 second of video is actually 10 seconds).

Movie S2.

Change in pain threshold to thermal stimulation pre- and post-administration of PD173212 in inflammatory pain model.

Data file S1. Raw data.

Provided as separate Excel file.